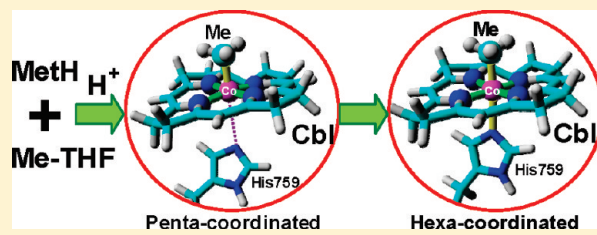


How Is a Co-Methyl Intermediate Formed in the Reaction of Cobalamin-Dependent Methionine Synthase? Theoretical Evidence for a Two-Step Methyl Cation Transfer Mechanism

Shi-Lu Chen,*^{†,‡} Margareta R. A. Blomberg,[‡] and Per E. M. Siegbahn*^{†,‡}[†]Key Laboratory of Cluster Science of Ministry of Education, Department of Chemistry, School of Science, Beijing Institute of Technology, Beijing 100081, P. R. China[‡]Department of Physics, Stockholm University, SE-10691 Stockholm, Sweden**S** Supporting Information

ABSTRACT: A methyl-Co(cobalamin) species has been characterized to be a crucial intermediate in the last step of the de novo biosynthesis of methionine catalyzed by cobalamin-dependent methionine synthase (MetH). However, exactly how it is formed is still an open question. In the present article, the formation of the methyl-Co(cobalamin) species in MetH has been investigated with B3LYP* hybrid DFT including van der Waals (vdW) interactions (i.e., dispersion) and using a chemical model built on X-ray crystal structures. The methyl cation and radical transfer mechanisms have been examined in various protonation states. The calculations reveal that the CH₃-Co(III)(cobalamin) formation in MetH proceeds along a stepwise pathway, where the first step is a methyl cation transfer from the protonated methyltetrahydrofolate (CH₃-THF) substrate to the Co(I)cobalamin. The second step is a binding of His759 to the other side (α -face) of Co. The former methyl transfer is computed to be the rate-limiting step with a barrier of 18 kcal/mol, which is reduced to 13 kcal/mol when dispersion is included. For the first step, the protonation at the methyl-bound nitrogen of CH₃-THF is very important. The methyl transfer is otherwise unreachable with a very high barrier of \sim 38 kcal/mol. The deprotonation of the α -face His759-Asp757-Ser810 triad is found to be much less significant but slightly facilitates the CH₃-Co(III)Cbl formation. There has been a long-standing discrepancy of 10–20 kcal/mol between theory and experiment in previous B3LYP computations of the Co-C bond dissociation energy for the methyl-Co(cobalamin) species. The calculations indicate that the lack of dispersion (\sim 11 kcal/mol) is the main origin of this puzzling problem. With these effects, B3LYP* gives a bond strength of 32 kcal/mol compared to the experimental value of 37 \pm 3 kcal/mol. Overall, the present calculations give many examples of dispersion that makes non-negligible contributions to the energetics of enzyme reactions, especially for systems involving at least one large reacting fragment approaching or departing.



INTRODUCTION

Cobalamin(Cbl)-dependent methionine synthase (MetH) is a methyltransferase responsible for the last step of the de novo biosynthesis of methionine (Met). It catalyzes the methyl transportation from methyltetrahydrofolate (CH₃-THF) to homocysteine (Hcy) to generate H-THF and methionine, using a cobalt(I) corrin cofactor, Co(I)Cbl, as a methyl carrier (Figure 1).^{1–4} MetH is a large modular enzyme generally composed of four distinct domains, Hcy, CH₃-THF, Cbl, and S-adenosylmethionine (AdoMet) binding domains. Between the Cbl binding domain and the other three domains, three methyl transfer processes take place. In the catalytic cycle (blue pathway in Figure 1), the Co(I)Cbl cofactor is reversibly methylated by CH₃-THF in the first half of the reaction, leading to a CH₃-Co(III)Cbl intermediate, and then demethylated by Hcy in the second half reaction. The third methyl transfer occurs between the Cbl and AdoMet binding domains in the repair of the occasionally inactivated Cbl cofactor (red pathway in Figure 1). Although the crucial CH₃-Co(III)Cbl species has

been confirmed by X-ray crystallography,⁵ exactly how it is formed is still an interesting open question. The investigation of the CH₃-Co(III)Cbl formation is thus of significance for the understanding of the MetH catalytic reaction and reactivation process.

MetH has been extensively characterized using a variety of mechanistic, kinetic, genetic, structural, and spectroscopic approaches. A number of X-ray crystal structures of MetH fragments have been deposited, such as the Hcy and CH₃-THF domains^{6,7} and the Cbl domain (Figure 2).⁵ In the active site of the CH₃-THF binding domain, the pterin ring of the CH₃-THF substrate is bound to Asn508, Asp473, Asn411, and Asp390 via hydrogen bonds. Among these residues, Asn508 interacts with the methyl-bound nitrogen of the substrate (N_m) and is suggested to play an important role in stabilizing the transition

Received: June 21, 2010**Revised:** January 23, 2011**Published:** March 21, 2011

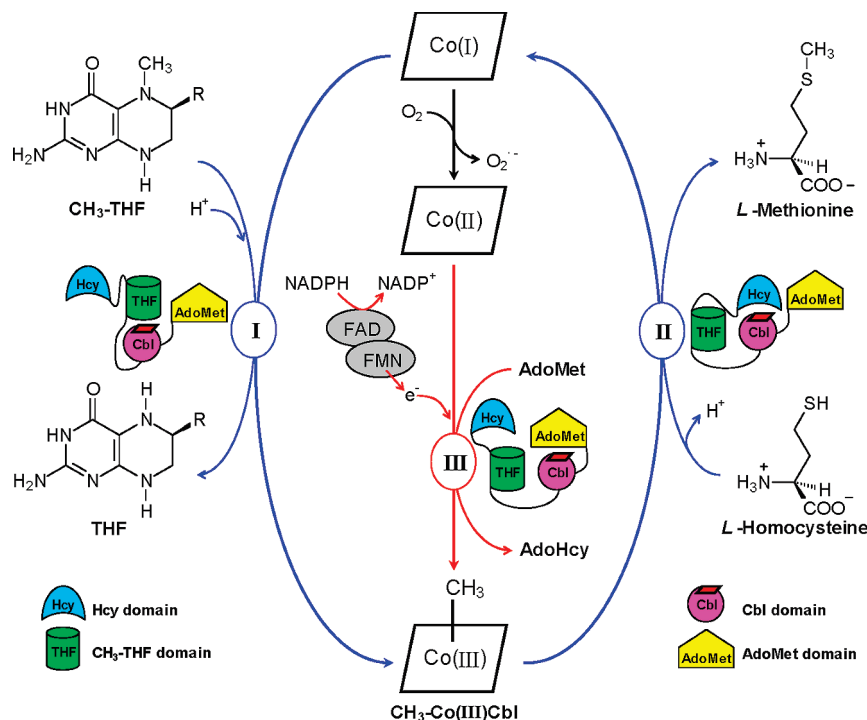
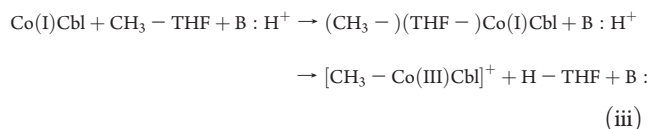
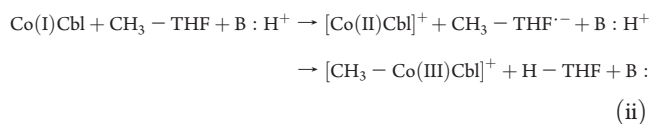
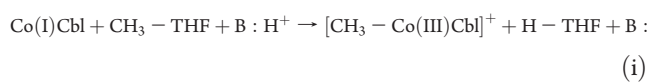


Figure 1. Catalytic cycle (blue) and reactivation reaction (red) of MetH. (I) The first half reaction. (II) The second half reaction. (III) The reactivation reaction. (AdoMet) S-adenosylmethionine. (AdoHcy) S-adenosylhomocysteine. (NADP^+) Nicotinamide adenine dinucleotide phosphate. (NADPH) The reduced form of NADP^+ . (FAD) Flavin adenine dinucleotide. (FMN) Flavin mononucleotide.

state or intermediate during methyl transfer.⁸ In the Cbl binding domain, the Cbl cofactor is docked into the protein by means of its various substituents. The ground-state Cbl in the active MetH has been revealed to be in a closed-shell Co(I) state⁹ with a square-planar tetracoordination at the Co atom.^{10,11} An axial ligand, the His759 in the α -face of Cbl (lower face in Figure 2), is bound to Co in the $\text{CH}_3\text{-Co(III)}\text{Cbl}$ intermediate. In contrast, the His759 is quite far away from cobalt in the Co(I)Cbl intermediate with a distance of 7.77 Å in an X-ray crystal structure of a MetH mutant fragment (PDB Code: 3BUL).¹² Upon methyl transfer to the β -face of Cbl (upper face in Figure 2), the Co becomes hexacoordinated by getting the additional His759 ligand from the His759-Asp757-Ser810 triad.⁵ Quite surprisingly, this rather dramatic motion has not been considered to play any major role for catalysis.^{12–15} Instead, the major role of His759 has been suggested to be in the control of the distribution of enzymatic conformations required for catalysis.^{12–15} The α - and β -faces of Cbl are both solvent-inaccessible in the MetH catalytic conformation, whereas in the reactivation conformation the β -face becomes solvent-accessible.¹⁵

Three possible mechanisms have been proposed for the first half reaction of MetH, i.e. (i) methyl cation transfer,^{1–4} (ii) single electron (methyl radical) transfer,⁴ and (iii) oxidative addition mechanisms.¹⁶



Mechanism (i) proceeds through a S_N2 -type pathway, that is direct methyl cation transfer, which requires the protonation at the N_m atom of $\text{CH}_3\text{-THF}$ to activate it.⁴ The timing of proton uptake relative to the methyl group movement is crucial, but still remains somewhat mysterious, since there is no obvious general acid (proton donor, “B:H⁺” in the equations above) near to the N_m atom,⁷ and the MetH(2–649) fragment (Hcy and $\text{CH}_3\text{-THF}$ domains) has been suggested to preferentially bind the unprotonated $\text{CH}_3\text{-THF}$.^{16,17} In fact, the crystal structure of the $\text{CH}_3\text{-THF}$ domain (PDB code: 1Q8J, Figure 2)⁷ shows a distance of 2.8 Å between the N_m and the side-chain nitrogen of the Asn508 and a much larger distance (4.1 Å) of the N_m to the side-chain oxygen of the Asn508, indicating that an unprotonated $\text{CH}_3\text{-THF}$ is bound by the protein with a hydrogen bond between the N_m and the Asn508 NH₂ group. However, it is difficult to differ between the nitrogen and oxygen ends of asparagine side chains, and the assignment might therefore be reversed, instead leading to the conclusion that $\text{CH}_3\text{-THF}$ would be protonated. Alternatively, the presence of the Cbl cofactor may be necessary for the $\text{CH}_3\text{-THF}$ activation and the proton transfer then probably takes place in the MetH(2–649)· $\text{CH}_3\text{-THF}$ ·Co(I)Cbl ternary complex.^{4,16,17} In mechanism (ii), an electron is transferred from the Co(I) atom to the $\text{CH}_3\text{-THF}$ substrate, followed by a methyl radical transfer from the substrate to the resulting Co(II)Cbl. However, the initial electron transfer appears to be thermodynamically unreachable.⁴ Mechanism (iii) includes a coordinating intermediate which has

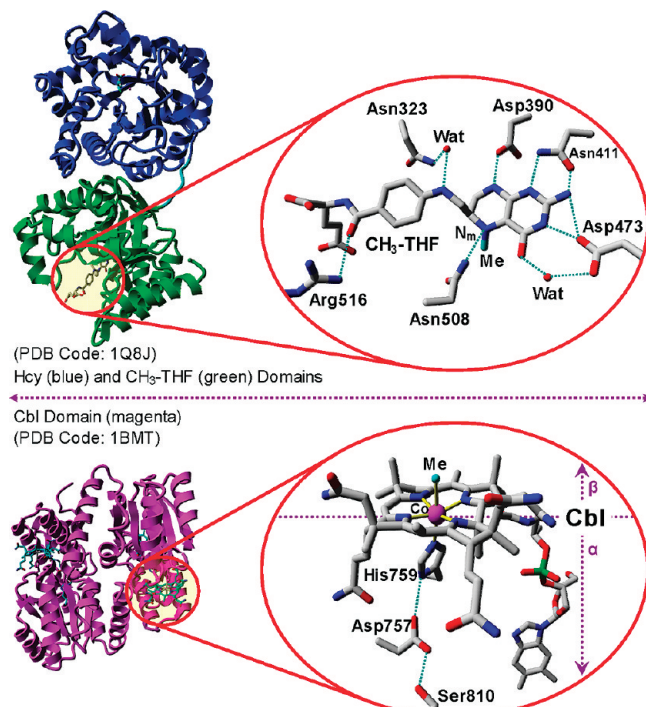


Figure 2. Overall structures of $\text{CH}_3\text{-THF}$ (upper) and Cbl (lower) domains and close-up views of their active sites. The transferred methyl is referred to as Me, the Me-bound nitrogen as N_m , and water molecules as Wat. The upper and lower faces of the Cbl factor are denoted by β and α , respectively. Hydrogen bonds are shown in cyan dashed lines.

a three-centered bond between the Co and the $\text{CH}_3\text{-N}$ moiety of the substrate, and the reaction leads to retention of configuration at the transferred methyl carbon (C_m). However, this mechanism suffers from the congested steric problem that the Cbl cofactor may be difficult to orientate close enough to both C_m and N_m of the substrate due to its bulky corrin macrocycle.^{1–4}

As presented above, in spite of the extensive studies, the $\text{CH}_3\text{-Co(Cbl)}$ formation mechanism of MetH is not fully understood yet and remains very attractive for biochemical studies. In the present work, we have investigated the mechanism for the first half reaction of MetH, using DFT with inclusion of dispersion (van der Waals effects), and with a chemical model constructed on the basis of the X-ray crystal structures of the $\text{CH}_3\text{-THF}$ (PDB Code: 1Q8J)⁷ and Cbl (PDB Code: 1BMT) domains.⁵ Because the oxidative addition mechanism is apparently unrealistic due to the serious congested steric problem,^{1–4} we will not discuss it any further, but rather focus on the mechanisms of methyl cation and radical transfer. We here present the energetics for the formation of the $\text{CH}_3\text{-Co(Cbl)}$ species in various protonation states and provide the characterization of the transition states and intermediates involved. Our calculations give a strong theoretical support for a two-step methyl cation transfer mechanism.

■ COMPUTATIONAL METHODS

All calculations were performed using unrestricted density functional theory (UDFT) with the hybrid functionals B3LYP^{18–20} and B3LYP* (further below). Some recalculations using restricted DFT have been made for optimized states without or with only little spin, and very similar energies were obtained.

Geometry optimizations of minima were carried out at the B3LYP level with the LACVP basis set as implemented in the *Jaguar 7.0* package.²¹ LACVP implies a 6-31G basis set^{22,23} for the first- and second-row elements and a nonrelativistic effective core potential²⁴ for the Co atom. Transition states were optimized at the B3LYP level with the LACVP basis set using the *Gaussian 03* package.²⁵ On the basis of these optimized geometries, more accurate energies were obtained using *Jaguar 7.0* by performing single-point calculations at both the B3LYP and B3LYP* levels with larger basis sets, that is laccv3p+ for Co and cc-pvtz(-f) for the other elements. To estimate the effects of the ignored protein environment on the calculated energies, solvation effects were calculated at the same theory level as the optimizations by performing single-point calculations on the optimized structures using the dielectric cavity method with a Poisson–Boltzmann solver,^{26,27} as implemented in *Jaguar 7.0*. The probe radius was set to 1.4 Å corresponding to the water molecule. The dielectric constant (ϵ) of the surrounding medium was chosen to be 4, which is a standard value that has been used in many previous studies.^{28–31} It is worth noting that, with respect to the polarizable continuum model (PCM), the solvation method used in the present work, which includes the total solute energy component (consisting of the nuclear–nuclear, electron–nuclear, kinetic, and two-electron terms), the total solvent energy component (computed as half of the total of the nuclear–solvent and electron–solvent terms), a solute cavity term, and the first-shell correction factor (depending on chemical functional groups in the molecule), gives similar results and would not change any conclusions about mechanisms. Using *Gaussian 03*, frequency calculations were performed at the same level of theory as the optimizations to obtain zero-point energies (ZPE) and to confirm the nature of the stationary points. The latter implies no negative eigenvalues for minima and only one negative eigenvalue for transition states. As described below, some atoms were kept fixed at their X-ray crystal positions. This procedure gives rise to a few small imaginary frequencies, which do not contribute significantly to the ZPE and should thus not affect the accuracy of the energies.

It is a common experience that, the DFT functional B3LYP*, for which the amount of Hartree–Fock exchange is reduced to 15% from 20% in the B3LYP functional,³² works better for transition metal containing systems.³³ In the present work, we employed both B3LYP and B3LYP* to evaluate the energetics by performing single-point calculations on the B3LYP-optimized geometries with the larger basis set described above. It is interesting to find that the B3LYP* energetics for the closed-shell Co–C association processes discussed below are very close to those obtained using B3LYP, even if cobalt still changes its oxidation state in those processes from Co(I) to Co(III). Nevertheless, for the open-shell homolytic Co–C bond cleavage processes, B3LYP* gives significantly better results than B3LYP (below), and for this reason B3LYP* results are used throughout this article. If not otherwise indicated, the energies reported in this article are calculated using B3LYP* and corrected for both solvation and zero-point vibrational effects. Because no gaseous molecule is introduced or generated during the reaction, entropy should not make significant contributions to the energetics and thus is not taken into account. In addition, absolute B3LYP and B3LYP* energies are both given in the Supporting Information.

Dispersion effects on the calculated energies are taken into account in the present enzyme system, where the reaction takes

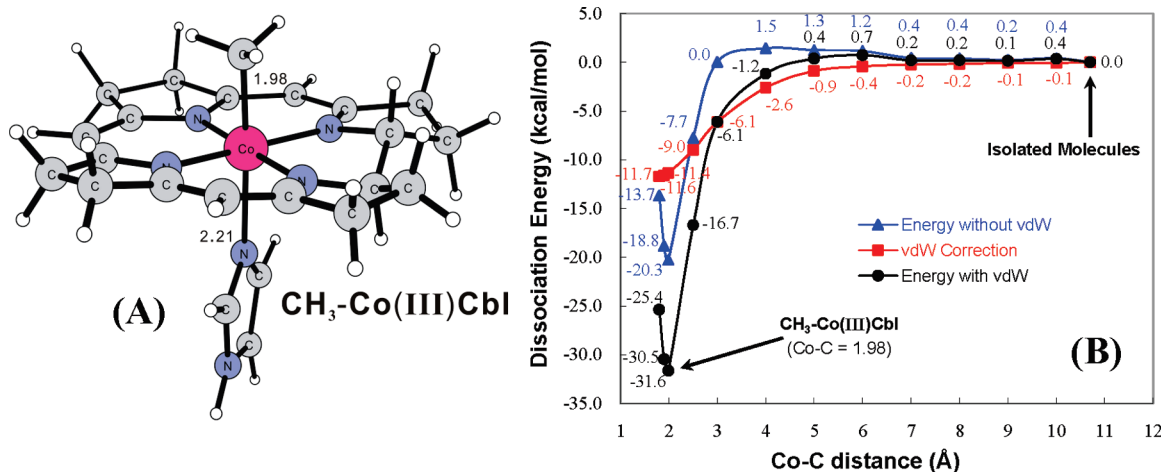


Figure 3. Optimized structure of the $\text{CH}_3\text{-Co(III)}\text{Cbl}$ species (A) and the Co–C bond dissociation energy (B). (vdW): van der Waals (dispersion). (Isolated Molecules): methyl radical and ${}^{\bullet}\text{Co(II)}\text{Cbl}$ are calculated separately. Energies are calculated using the B3LYP* functional including ZPE and solvation effects. In addition, a diagram for the B3LYP Co–C BDE (Figure S1) is given in the Supporting Information.

place between the two massive species, that is $\text{CH}_3\text{-THF}$ and Cbl. The dispersion corrections were calculated by performing single-point calculations on the optimized structures using an empirical formula by Grimme,^{34,35} as programmed in the ORCA package.³⁶

RESULTS AND DISCUSSION

Validation of Method for the Co–C Bond Strength. In a few studies, it was shown that the nonhybrid BP86 functional gave $(\text{Cbl})\text{Co-C(alkyl)}$ bond dissociation energies (BDE) closer to the experimental values than hybrid functionals such as B3LYP, and it was proposed that BP86 should be more reliable than the B3LYP functional for Cbl-dependent systems.^{37–40} However, no van der Waals (vdW) effects (i.e., dispersion) inside the reacting cores were considered in those investigations. Rather, recently it has been realized that the lack of dispersion in DFT theory can lead to large effects when atoms are forced closer to each other, especially for systems with large substituents or ligands.⁴¹ In the article published recently,⁴¹ it has been demonstrated that it is essentially the lack of the dispersion correction that led to the long-standing problem of hybrid DFT in the prediction of the Co–C BDE for $\text{CH}_3\text{-Co(Cbl)}$, where the B3LYP hybrid functional always underestimated the BDE by 10–20 kcal/mol depending on the computational details.^{37–44} Using a model shown in part A of Figure 3, a Co–C BDE for $\text{CH}_3\text{-Co(Cbl)}$ in ethylene-glycol ($\varepsilon = 40$) was reported to be 32 kcal/mol with a dispersion correction of ~11 kcal/mol at the B3LYP* level of theory (including zero-point and solvent corrections).⁴¹ The detailed energy curves for the Co–C bond dissociation are now shown in part B of Figure 3.

It is worth noting that, with the inclusion of dispersion (~11 kcal/mol), the homolytic Co–C BDE for $\text{CH}_3\text{-Co(Cbl)}$ obtained in B3LYP calculations is 27.5 kcal/mol (Figure S1 in the Supporting Information), still rather far from the experimental value of 37 ± 3 kcal/mol.^{45,46} However, the B3LYP* value of 32 kcal/mol (part B of Figure 3 and ref 41) is quite close to the experiment. This improvement in the Co–C BDE prediction with the decrease of Hartree–Fock exchange in the functional implies that, besides the lack of dispersion, also inherent errors in the B3LYP functional contribute to the problem in the Co–C

BDE prediction for $\text{CH}_3\text{-Co(Cbl)}$. The present calculations show that the use of B3LYP* makes up for most of this kind of the error (~5 kcal/mol), although a few effects (5 ± 3 kcal/mol) are still missing.

The increase in the Co–C BDE prediction with the decrease of Hartree–Fock exchange in the functional is consistent with the finding in the previous studies that the nonhybrid BP86 functional gives stronger Co–C BDE than B3LYP.^{37–40} However, because the BP86 calculations would lead to the same dispersion corrections as the ones in the present article produced by B3LYP due to the same parameters for BP86 and B3LYP in the empirical dispersion method,^{34,35} the inclusion of dispersion would significantly increase the BP86-computed Co–C BDE in the previous BP86 investigations^{37–40} and make it unreasonably high. Therefore, the employment of BP86 appears to utilize the exaggerated binding energy evaluation to cover the lack of dispersion in calculations of Cbl-dependent systems. The method employed in the present work, that is the use of the B3LYP* functional coupled with empirical dispersion corrections, should therefore be a better choice for theoretical investigations of Cbl-dependent enzyme reactions.

In general, it can be concluded that dispersion (vdW effects) can make non-negligible contributions to the energetics of bond cleavage processes and should be included in energy calculations of enzymatic catalysis, particularly for the reactions involving interactions where at least one of the reacting fragments is large. Furthermore, the empirical method developed by Grimme^{34,35} has been shown to work quite well in the description of the covalent Co–C bond dissociation and formation. The calculations which continue to a shorter Co–C distance (Co–C = 1.9 and 1.8 Å) in the present $\text{CH}_3\text{-Co(Cbl)}$ system shows a minimum at the optimum distance of 1.98 Å (Figure 3 and Figure S1 of the Supporting Information). This gives a further indication that the present methodology with dispersion included performs very well at a bonded distance, not only at a long-range distance.

Chemical Model. A chemical model including the active sites of the Cbl and $\text{CH}_3\text{-THF}$ domains in MetH was built on the basis of two X-ray crystal structures (Figure 4). Because there is no structure available which comprises both Cbl and $\text{CH}_3\text{-THF}$ domains, we used the coordinates from the PDB entries 1BMT⁵

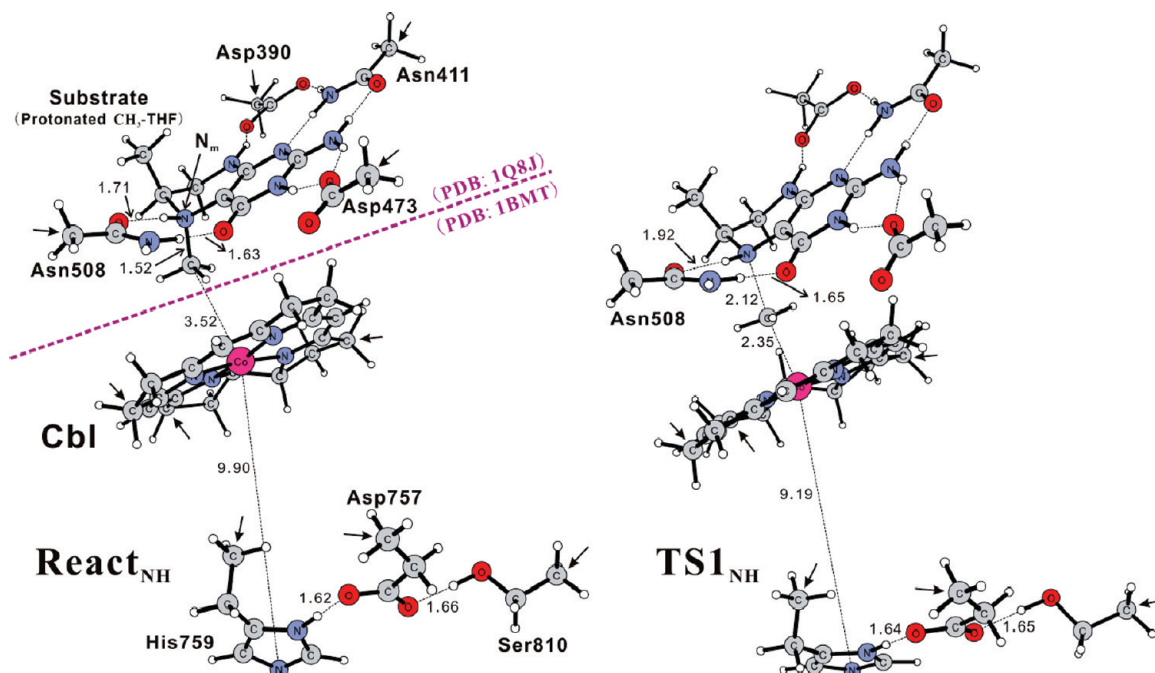


Figure 4. Optimized structures of the MetH enzyme–substrate complex (**React_{NH}**) and the transition state for methyl cation transfer (**TS1_{NH}**) in the **NH** protonation state, which denotes that the N_m atom is protonated and the Asp757 residue is deprotonated. The parts above and below the pink dashed line are extracted from PDB entries 1Q8J (7) and 1BMT (5), respectively. Arrows indicate the atoms that are fixed in the optimizations. All distances are given in angstroms (Å).

and 1Q8J⁷ to generate the Cbl and CH₃–THF binding sites, respectively. The Cbl binding part contains the Cbl cofactor and the His759-Asp757-Ser810 triad. To reduce the size, some truncations have been made. All substituents in cobalamin were replaced by hydrogens, whereas the His759, Asp757, and Ser810 residues were represented by ethyl-imidazole, propionate, and ethanol, respectively. The terminal carbons of the triad and three carbons in the Cbl macrocycle, where the truncations have been done, were fixed to their X-ray crystal positions in all optimizations. Among 10 possible atoms in the Cbl macrocycle, any 3 carbons that are located at different pyrrole rings can be selected but should not be changed throughout the investigation. The CH₃–THF binding part consists of a CH₃–THF substrate and the Asp390, Asn411, Asp473, and Asn508 amino acids. Some truncations have also been applied to this part, that is the long chain of the substrate was replaced by a methyl, whereas the aspartates and asparagines were cut out as acetates and acetamides, respectively. A proton was placed at the N_m atom of the substrate to simulate the protonated CH₃–THF, whereas the Asp757 in the Cbl binding part was deprotonated, which is referred to as the **NH** protonation state in the present article. In the **NH** protonation state, the total charge of the model is –2 and the total number of atoms is 139.

To attain more reasonable structures, we first optimized the transition state (TS) for the methyl transfer in the **NH** protonation state (**TS1_{NH}**, Figure 4), rather than doing this for the enzyme–substrate complex. **TS1_{NH}** was optimized without locking any atom in the CH₃–THF binding part, but keeping the fixation in the Cbl binding site. Once the optimized geometry of **TS1_{NH}** was obtained, the terminal carbons of the four residues in the CH₃–THF binding site were frozen in their optimized positions to optimize the enzyme–substrate complex (**React_{NH}**, Figure 4) and other subsequent stationary points. This optimization

procedure is also applied to the reactions in the other protonation states discussed below. Without this procedure (the CH₃–THF binding part is completely free in optimizations), different orientations of the CH₃–THF group relative to the Cbl will be produced when the starting conformations are different. With the CH₃–THF binding part free, we tried a number of different starting conformations and found that, in all resulting orientations, the distances of atoms in the CH₃–THF binding site to those in the Cbl were never shorter than 2.4 Å. This indicates that, in the present model, the interactions between the CH₃–THF and Cbl binding sites are weak and energies of all conformations must be similar. Indeed, energy evaluations show that energy differences between all conformations and the **React_{NH}** (obtained using the procedure described above) are always within 2.4 kcal/mol (5 kcal/mol with dispersion included). It should be admitted here that some of those energy changes would increase the activation energy. However, considering the reaction barrier obtained in this article (13 kcal/mol with dispersion included, discussed in next section), energy changes of this amount will not modify any conclusions about mechanisms.

In the **NH** protonation state, the overall geometrical parameters obtained from the geometry optimization of the present model of the MetH active sites agree well with experiments and previous calculations. For example, in the **React_{NH}**, the distances of Co to the four ligated nitrogens of Cbl are calculated to be 1.92, 1.92, 1.86, and 1.86 Å, to be compared to the crystallographic values 1.98, 1.91, 1.84, and 1.85 Å,⁵ the PBE-computed distances 1.91, 1.91, 1.84, and 1.84 Å,⁹ and the EXAFS (Extended X-ray absorption fine structure)-fitted average distance 1.86–1.88 Å.^{10,11} The protonated CH₃–THF substrate is oriented by four hydrogen-bonding residues at a position reasonably close to the Cbl cofactor. The distance of the Co to the carbon of the

Table 1. Properties of Stationary Points in the $\text{CH}_3\text{—Co(Cbl)}$ Formation of MetH

entry	complex ^a	spin/charge			energy ^d (kcal/mol)
		Co	N_m^b	C_m^c	
1	React _{NH}	0.00/0.28	0.00/−0.71	0.00/−0.29	0.0 (0.0)
2	TS1 _{NH}	−0.08/0.30	0.02/−0.67	0.05/−0.32	18.0 (13.1)
3	Int1 _{NH}	0.00/0.37	0.00/−0.70	0.00/−0.39	6.2 (2.9)
4	TS2 _{NH}	0.00/0.37	0.00/−0.71	0.00/−0.38	10.5 (1.5)
5	Int2 _{NH}	0.00/0.34	0.00/−0.72	0.00/−0.37	5.8 (−7.6)
6	React _N	0.00/0.31	0.00/−0.54	0.00/−0.28	0.0 (0.0)
7	TS1 _N	0.00/0.30	0.00/−0.49	0.00/−0.38	46.1 (38.4)
8	Int1 _N	0.00/0.40	0.00/−0.47	0.00/−0.42	44.3 (43.8)
9	Int1b _N	0.00/0.40	0.57/−0.46	0.00/−0.42	30.4 (30.6)
10	TS2 _N	0.00/0.40	0.57/−0.44	0.00/−0.40	41.2 (35.0)
11	Int2 _N	−0.01/0.37	0.57/−0.45	0.00/−0.39	36.0 (24.1)
12	React _{NHP}	0.00/0.26	0.00/−0.70	0.00/−0.30	0.0 (0.0)
13	TS1 _{NHP}	−0.11/0.28	0.03/−0.66	−0.07/−0.32	19.6 (15.7)
14	Int1 _{NHP}	0.00/0.38	0.00/−0.71	0.00/−0.40	6.3 (4.5)
15	TS2 _{NHP}	0.00/0.38	0.00/−0.74	0.00/−0.37	12.5 (3.3)
16	Int2 _{NHP}	0.00/0.35	0.00/−0.75	0.00/−0.37	7.1 (−7.1)
17	React _{NH} (T)	1.10/0.55	0.00/−0.71	0.00/−0.30	8.4 (8.6)
18	TS1 _{NH} (T)	0.86/0.45	0.32/−0.63	−0.52/−0.42	39.8 (36.9)
19	Int1 _{NH} (T)	0.00/0.42	0.37/−0.68	0.00/−0.44	23.3 (23.9)
20	TS2 _{NH} (T)	0.00/0.41	0.37/−0.68	0.00/−0.42	34.5 (28.9)
21	Int2 _{NH} (T)	0.01/0.38	0.37/−0.68	0.00/−0.41	29.2 (18.3)

^a Abbreviations signify reacting state (React), TS for methyl transfer (TS1), pentacoordinated $\text{CH}_3\text{—Co(Cbl)}$ intermediate (Int1), pentacoordinated $\text{CH}_3\text{—Co(Cbl}^\bullet\text{)}$ radical (Int1b), TS for His759 nitrogen binding (TS2), and hexacoordinated $\text{CH}_3\text{—Co(Cbl)}$ intermediate (Int2); subscripts indicate the different protonation substrates; (T): Triplet state. ^b The methyl-bound nitrogen of the substrate. ^c The carbon of the transferred methyl. ^d The energies are calculated using the B3LYP* functional including ZPE and solvation effects, while the ones with dispersion (vdW effects) included are given in parentheses.

transferred methyl (C_m) is 3.52 Å. It can be noticed that His759 is positioned very far away from the Cbl with a N–Co distance of 9.90 Å. This long distance is reasonable, since a corresponding N–Co distance of 7.77 Å in an X-ray crystal structure of a MetH mutant fragment (PDB Code: 3BUL)¹² shows that the α -face ligand (His759) is quite flexible and the N–Co distance can be very long in this very complicated enzyme. A further investigation, scanning the N–Co distance from 9.90 to 2.33 Å, indicates that the energy of the complex is hardly changed in the distance range of 9.90–6.00 Å with dispersion considered (Figure S2 in the Supporting Information). When the N–Co distance is shorter than 6.00 Å, the energy is raised to a value as high as 23 kcal/mol (13 kcal/mol with dispersion included) for an N–Co distance of 2.33 Å. The optimized enzyme–substrate complex (**React_{NH}**) is found to be in a closed-shell Co(I) state without any unpaired spin and a charge of 0.28 at the Co atom (entry 1 in Table 1). We also obtained a complex in the open-shell singlet state, formed by antiferromagnetic coupling between Co(II) (spin = 0.75) and a corrin radical (geometry in Supporting Information). Its energy is 0.3 kcal/mol higher than the closed-shell singlet complex of Figure 4. This is not very different from Jensen's study,⁴⁷ where they found a similar open-shell singlet state 1 kcal/mol lower than the closed-shell singlet state using a small model (only containing Co and corrin macrocycle). As pointed out by Jensen and Ryde,⁴⁷ energy differences of this amount are within the uncertainty of the method. Therefore, it is not safe to say which state definitely is the ground state. Considering that the ground state of the Co(I)Cbl cofactor has been stated to be in a

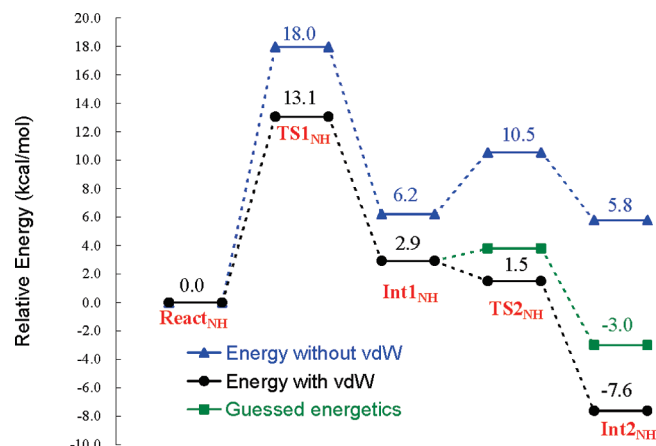


Figure 5. Schematic potential energy profile for the $\text{CH}_3\text{—Co(III)Cbl}$ formation in the NH protonation state. (vdW): van der Waals (dispersion). Energies are calculated using the B3LYP* functional including ZPE and solvation effects. See text for definition of the guessed energies.

closed-shell singlet state by spectroscopic techniques,⁹ we use the closed-shell enzyme–substrate complex (**React_{NH}**, Figure 4) as the ground state in discussions of the present article.

Methyl Cation Transfer Mechanism. As mentioned above, a transition state (TS1_{NH}, Figure 4) for the methyl transfer from the protonated $\text{CH}_3\text{—THF}$ substrate to Co, which is connected

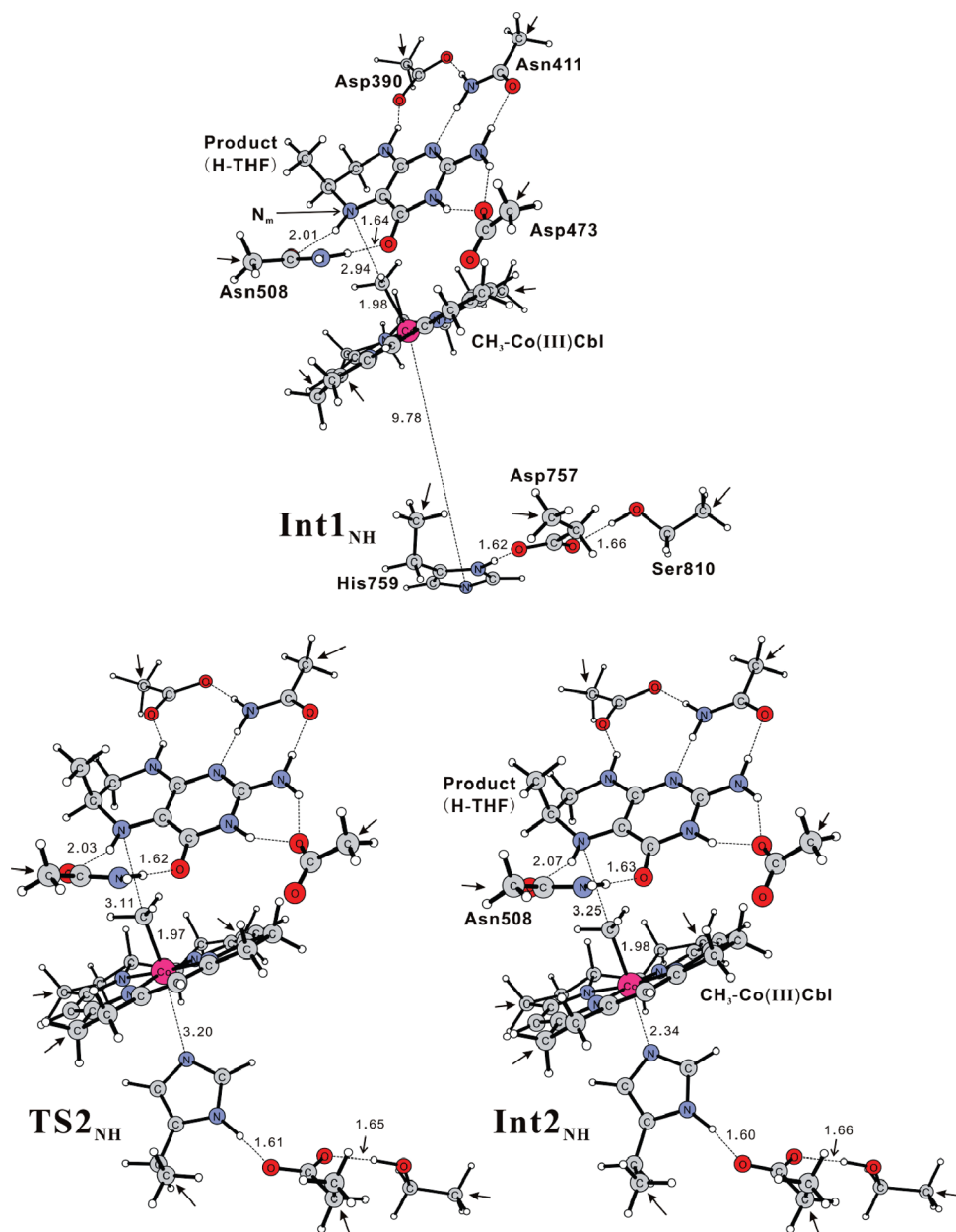


Figure 6. Optimized structures of the pentacoordinated $\text{CH}_3\text{-Co(III)}\text{Cbl}$ intermediate (Int1_{NH}), the transition state for the His759 binding (TS2_{NH}), and the resulting hexacoordinated $\text{CH}_3\text{-Co(III)}\text{Cbl}$ intermediate (Int2_{NH}) in the NH protonation state.

to the React_{NH} along the reaction pathway, has been optimized. The nature of TS1_{NH} has been confirmed to be a first-order saddle point with an imaginary frequency of $437i \text{ cm}^{-1}$, where the $\text{Co}-\text{C}_m$ bond is formed simultaneously with the C_m-N_m bond breaking. At TS1_{NH} , the key distances of the methyl carbon to the N_m (C_m-N_m) and Co ($\text{Co}-\text{C}_m$) are 2.12 and 2.35 Å, respectively. The methyl group is determined to be a cation (entry 2 in Table 1). With solvation effects of the surrounding protein included, the calculated barrier for this step is 18 kcal/mol (entry 2 in Table 1 and the schematic potential energy profile in Figure 5). When dispersion are added, the barrier for the methyl cation transfer is reduced to ~ 13 kcal/mol (Figure 5 and entry 2 in Table 1), which is well in line with the experimental rate constant ($\sim 7 \times 10^4 \text{ mol}^{-1}\text{s}^{-1}$)⁴⁸ and reproduces the effect of the reaction acceleration by the MetH enzyme.

The methyl transfer leads to a pentacoordinated $\text{CH}_3\text{-Co(Cbl)}$ intermediate (Int1_{NH} , Figure 6), which is found to lie ~ 6 kcal/mol (~ 3 kcal/mol with dispersion included, Figure 5 and entry 3 in Table 1) higher than the React_{NH} . The increased charges at the Co (0.37) and C_m (-0.39) atoms and their unchanged spin populations (both zero) show that this $\text{CH}_3\text{-Co(Cbl)}$ species is in a closed-shell $\text{CH}_3\text{-Co(III)}\text{Cbl}$ state. In Int1_{NH} , the $\text{Co}-\text{C}_m$ bond distance is calculated to be 1.98 Å, which is in excellent agreement with the crystallographic value of 1.98 Å,⁴⁹ the previous DFT-computed distance of 1.99 Å,⁵⁰ and the QM/MM (Quantum mechanics/molecular mechanics method)-computed distance of 1.97 Å.⁴² An interesting observation here is that, in going from React_{NH} to Int1_{NH} via TS1_{NH} (Figures 4 and 6), the distance of the Asn508 oxygen to the N_m -binding proton is elongated from 1.71 Å to 2.01 Å (1.92 Å at

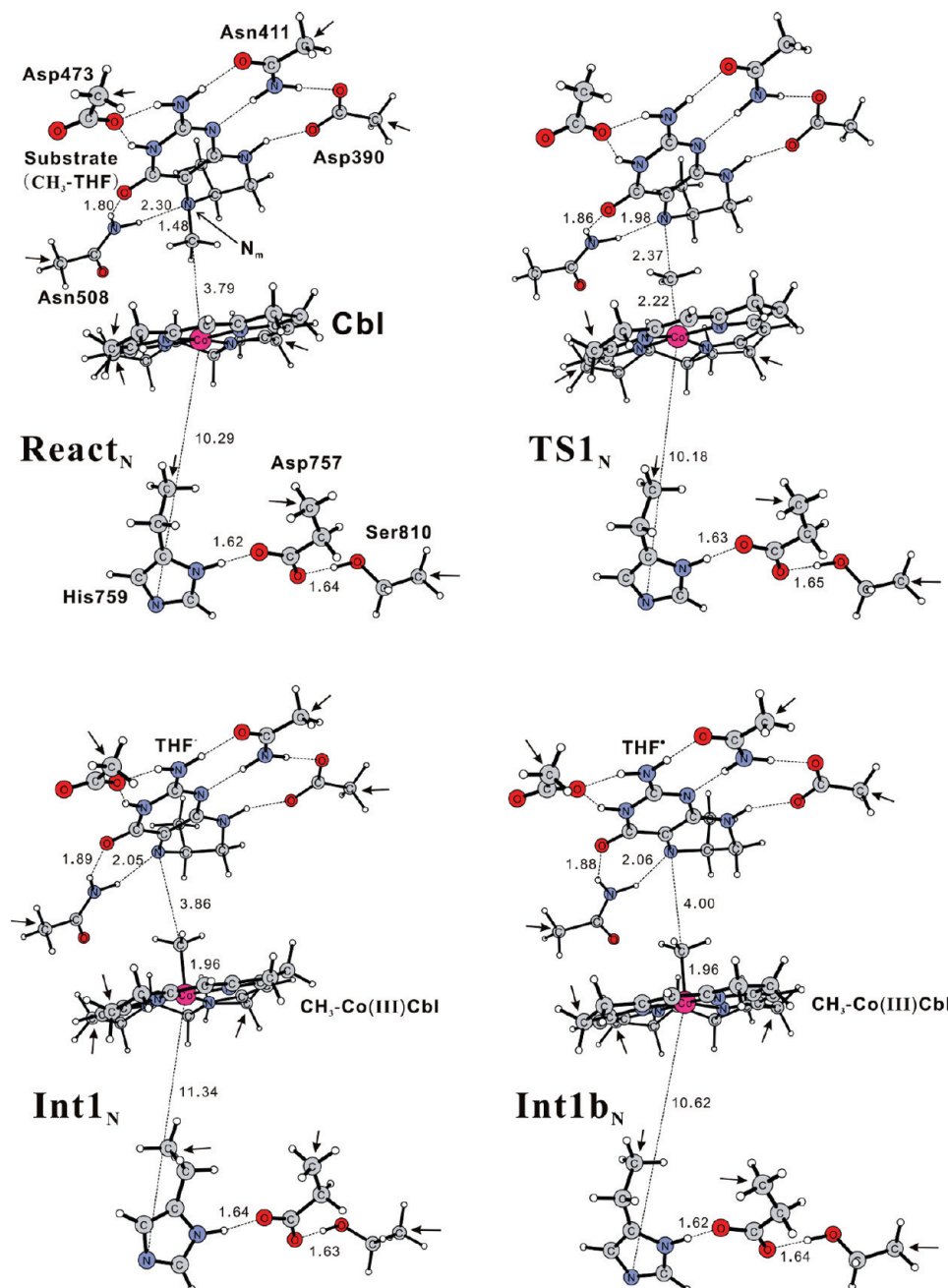


Figure 7. Optimized structures of the MetH enzyme–substrate complex (**React_N**), the following TS for methyl cation transfer (**TS1_N**), and the resulting pentacoordinated closed-shell $\text{CH}_3\text{-Co(III)}\text{Cbl}$ intermediate (**Int1_N**) and singlet open-shell $\text{CH}_3\text{-Co(III)}(\text{Cbl}^*)$ radical (**Int1b_N**) in the *N* protonation state, which implies that the N_m atom of the substrate is unprotonated and Asp757 is deprotonated.

TS1_{NH}). This indicates that the Asn508 plays a role in stabilizing the transition state (**TS1_{NH}**) and the intermediate (**React_{NH}**) in the reverse reaction, that is a methyl cation transfer from Co to the neutral H–THF. Because the **React_{NH}**, in which the $\text{CH}_3\text{-THF}$ substrate is already protonated, probably is an intermediate for the Michaelis complex (where the substrate is unprotonated) in the real case, this stabilization provided by Asn508 may be of significance for the reversible methyl transfer in the first half reaction of MetH, in line with suggestions from the mutation experiment.⁸

In the second step of the mechanism (Figure 5), from **Int1_{NH}** overcoming a small barrier of 4.3 kcal/mol, the His759 nitrogen

coordinates to the Co, leading to a hexacoordinated $\text{CH}_3\text{-Co(Cbl)}$ species (**Int2_{NH}**, Figure 6). The transition state for His759 binding (**TS2_{NH}**, Figure 6) is calculated to have a distance of 3.20 Å between the Co and the His759 nitrogen. This binding slightly lowers the energy of the complex by 0.4 kcal/mol but hardly changes any electronic properties (entries 3 and 5 in Table 1). However, the addition of dispersion corrections leads to a considerable decrease in energy for the His759 binding, which seems to make the $\text{CH}_3\text{-Co(Cbl)}$ formation irreversible (Figure 5). This large effect may be attributed to the association between the Co and the “free” His759, the latter approaching the massive Cbl from a position ~10 Å away from the Co (Figure 6). However, it should be realized that, in the

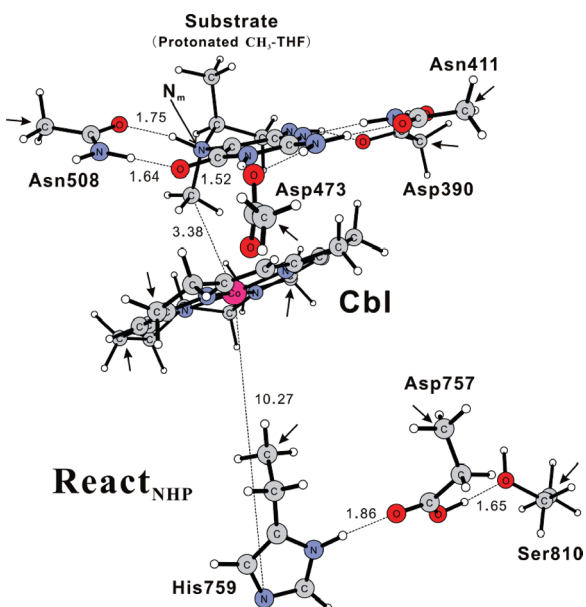


Figure 8. Optimized structure of the MetH enzyme–substrate complex (**React_{NHP}**) in the *NHP* protonation state, which indicates that both the N_m atom and Asp757 are protonated.

real environment, the His759 would not be “free” and must be bound more tightly to other residues, or (and) the main chain of the protein, not included in the present model. In an X-ray crystal structure of a mutant fragment (PDB Entry: 3BUL),¹² His759 interacts with the adjacent AdoMet domain via a hydrogen bond to the Asp1093 and a water-mediated hydrogen bond to the Glu1069. If these interactions between His759 and other groups would be taken into account, the energies of the enzyme–substrate complex, the TS for methyl transfer, and the pentacoordinated $\text{CH}_3\text{--Co}(\text{Cbl})$ intermediate should all be lowered, thus making the energetics of His759 binding more reasonable. The lowering effect of -13.4 kcal/mol for the **Int2_{NH}** (Figure 5) is therefore probably exaggerated. However, it should be emphasized that, due to the quite complicated conformational changes during the MetH reaction and the limited crystal structures available, it is very difficult to model the His759 binding step with precise interactions included. This would certainly be true even if a QM/MM method was employed. Many attempts were made to simulate the His759 binding with more residues included, but these always led to unreliable structures. Thus, an assumption is instead made as follows. Because the **Int2_{NH}** can be observed in experiments but the **React_{NH}** could not, the former should be at least ~ 3 kcal/mol lower than the latter according to the Boltzmann distribution. To keep the whole process reversible, -3 kcal/mol may thereby be a reasonable value for the energy of the hexacoordinated $\text{CH}_3\text{--Co}(\text{Cbl})$ intermediate (Figure 5).

In summary, the formation of the hexacoordinated $\text{CH}_3\text{--Co}(\text{Cbl})$ intermediate in the *NH* protonation state proceeds along a stepwise pathway, i.e. the methyl cation transfer from the protonated $\text{CH}_3\text{--THF}$ substrate to the Co is followed by the binding of the His759 nitrogen. With dispersion added, the methyl cation transfer is predicted to be the rate-limiting step with a barrier of ~ 13 kcal/mol for the forward reaction direction (Figure 5). As discussed above, the reverse direction should have a probable barrier of ~ 16 kcal/mol (with inclusion of dispersion), showing that the methyl transfer in the first half reaction of MetH is reversibly accessible when the $\text{CH}_3\text{--THF}$ substrate gets protonated at its N_m atom. Many attempts were

made to locate a concerted transition state where the methyl cation transfer should occur simultaneously with the His759 binding, but without success. With inclusion of possible missing hydrogen bonding to the released His759, this concerted mechanism would be even less likely.

Timing of Proton Uptake. Because the H--THF product includes a proton at the N_m atom, this protonation is thought to be important for the first half reaction of MetH. The timing of proton uptake with respect to the methyl transfer is thus a very interesting and critical issue for the $\text{CH}_3\text{--Co}(\text{Cbl})$ formation in MetH. Although we have proved the feasibility of the methyl transfer with the protonation at N_m , it is still worth examining the possibility without this protonation, as the comparison between them would offer direct evidence for the timing of proton uptake. To test that, we removed the proton at N_m from the *NH* protonation state (this new protonation state is referred to as the *N* protonation state, Figure 7) and reoptimized the stationary points along the methyl transfer pathway.

It is found that the hexacoordinated $\text{CH}_3\text{--Co}(\text{Cbl})$ formation in the *N* protonation state follows a comparable pattern to the case in the *NH* protonation state, and similar stationary points have been located (Figure 7 and Supporting Information for geometries and Table 1 for properties). In the *N* protonation state, with a closed-shell enzyme–substrate complex (**React_N** in Figure 7 and entry 6 in Table 1) as the starting point, the methyl group is delivered to Co from the neutral $\text{CH}_3\text{--THF}$, resulting in an open-shell complex of a pentacoordinated $\text{CH}_3\text{--Co}(\text{Cbl}^\bullet)$ intermediate with a THF^\bullet radical (**Int1b_N** in Figure 7 and entry 9 in Table 1), which is actually lower in energy than the closed-shell complex of a pentacoordinated $\text{CH}_3\text{--Co}(\text{III})\text{Cbl}$ species with a negatively charged THF (**Int1_N** in Figure 7 and entry 8 in Table 1, see the detailed discussion in the next paragraph). The transition state for this step (**TS1_N**, Figure 7) has been optimized and calculated to have an imaginary frequency of $517i\text{ cm}^{-1}$. The closed-shell character of the methyl carbon (Table 1, entry 7) in **TS1_N** clearly shows that this is a process of methyl cation transfer. However, this step is predicted to be strongly endothermic by ~ 44 kcal/mol (~ 44 kcal/mol with dispersion included, entry 8 in Table 1), with a very high barrier of ~ 46 kcal/mol (~ 38 kcal/mol with dispersion included, entry 7 in Table 1). Consistent with the energetics, the optimized **TS1_N** is rather late with a very short Co–C_m distance of 2.22 \AA (Figure 7). This unambiguously indicates that, without the protonation at the $\text{CH}_3\text{--THF}$ substrate, the methyl transfer for the $\text{CH}_3\text{--Co}(\text{Cbl})$ formation in MetH is unreachable. Coupled with the results in the *NH* protonation state presented above, it can thus be concluded that the proton uptake in the first half reaction of MetH must take place before or simultaneously with the methyl transfer, rather than after that, as suggested previously.⁴ However, the cost of the protonation of the substrate is difficult to calculate in the present study, because the source of proton and protonation process are still unclear experimentally. Although the pK_a of the free $\text{CH}_3\text{--THF}$ substrate in aqueous solution has been determined to be 5.05 ,¹⁶ it is not unlikely that it is increased to above 7 by the protein surrounding. For example, the substrate ring is bound by two aspartate and two asparagine residues (Figures 2 and 4), among which the Asn508 was suggested to stabilize the protonated substrate (the discussion above),⁸ facilitating the protonation of the substrate. In addition, it was shown that the presence of the Cbl cofactor may be necessary for the substrate activation and the proton uptake then probably takes place in the $\text{MetH}(2-649)\cdot\text{CH}_3\text{--THF}\cdot\text{Co}(\text{I})\text{Cbl}$

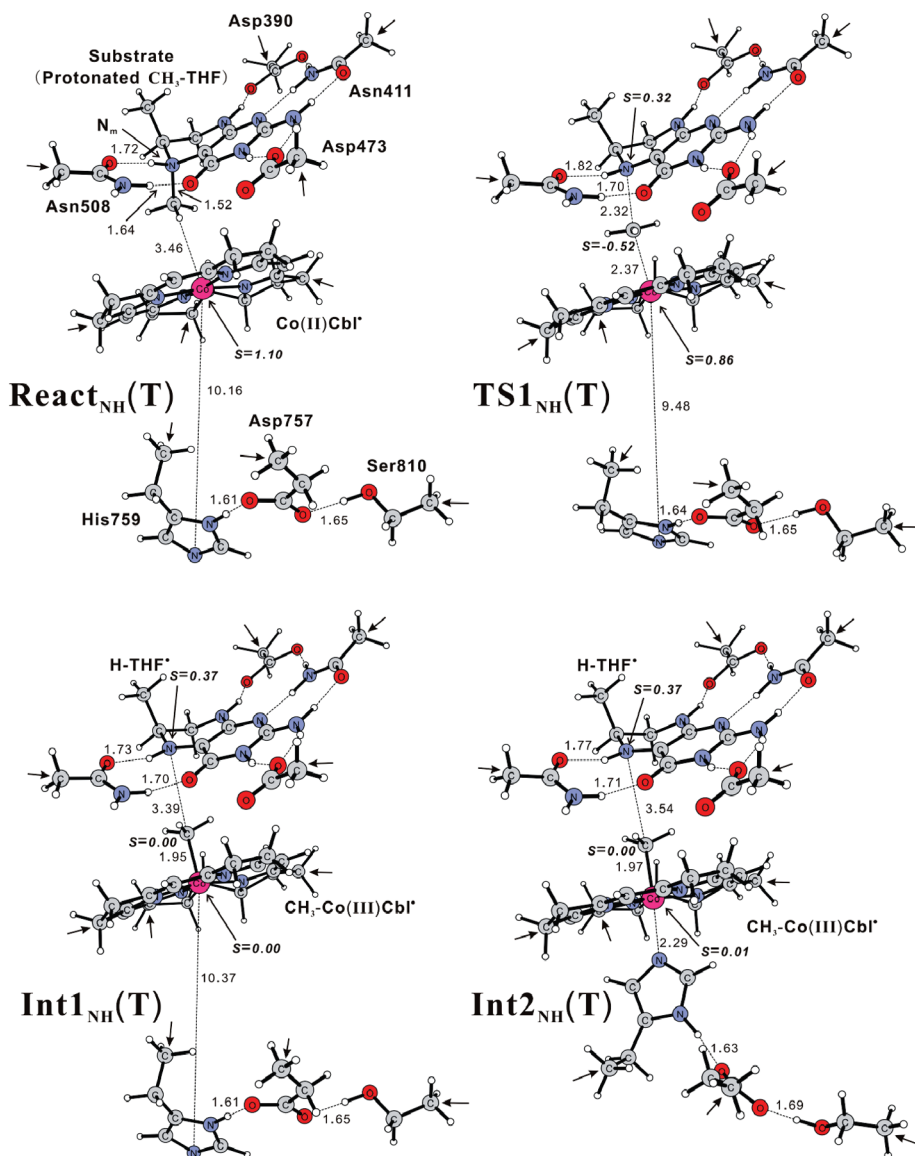


Figure 9. Optimized triplet-state structures of the MetH enzyme–substrate complex (**React_{NH}(T)**), the following TS for methyl radical transfer (**TS1_{NH}(T)**), and the resulting penta- (**Int1_{NH}(T)**) and hexacoordinated (**Int2_{NH}(T)**) CH₃–Co(III)(Cbl[•]) intermediates in the *NH* protonation state. The unpaired spin populations are shown also. The TS for His759 binding is given in the Supporting Information.

ternary complex,^{4,16,17} indicating that the cost of protonation is probably compensated by the conformation change of the enzyme. In any case, the cost should be very small. Furthermore, it is also very difficult to accurately calculate the energy cost of protonation, even though the pK_a value of the free substrate in aqueous solution is available.

It is interesting to note that the open-shell pentacoordinated CH₃–Co(Cbl[•]) intermediate (**Int1b_N**) turns out to derive from a closed-shell pentacoordinated CH₃–Co(III)Cbl species (**Int1_N**) through a single electron transfer from the negatively charged THF to the π* orbital of the corrin macrocycle, the lowest unoccupied molecular orbital (LUMO) of CH₃–Co(III)Cbl.⁵¹ This closed-shell pentacoordinated CH₃–Co(III)Cbl species is calculated to be ~14 kcal/mol (~13 kcal/mol with dispersion included) higher than the open-shell **Int1b_N** (Table 1, entries 8 and 9). Although it is practically unfeasible to reach these two states due to the impossibility of the methyl transfer in the *N* protonation state, this unexpectedly provides a

theoretical analogue to a recently proposed scheme for the second half reaction of MetH, in which a singlet open-shell complex of a CH₃–S[•] radical with a pentacoordinated CH₃–Co(III)(Cbl[•]) radical has been shown to be energetically lower than a closed-shell complex of CH₃–S[−] with CH₃–Co(III)–(Cbl).⁵² From the **Int1b_N**, the following TS for the His759 binding (**TS2_N**) and the resulting hexacoordinated CH₃–Co(III)(Cbl[•]) intermediate (**Int2_N**) have also been obtained and their geometries and properties are given in the Supporting Information and in Table 1, respectively.

Effect of Protonation State in the His759-Asp757-Ser810 Triad. It has been proposed that a proton is released to solvent from the His759-Asp757-Ser810 triad with the CH₃–Co(Cbl) formation in MetH and the deprotonation at the triad must increase the basicity of His759, thereby helping the stabilization of the CH₃–Co(Cbl) intermediate.⁵ It is thus worth knowing how the protonated triad functions in the formation of CH₃–Co(Cbl) intermediate, as this would give further understanding

of the effect of the protonation state in the triad. Therefore, we added a proton to the Asp757 in the *NH* protonation state keeping the proton at N_m (this state is called the *NHP* protonation state, Figure 8), and then followed the reaction pathway for the CH₃–Co(Cbl) formation. Not unexpectedly, our calculations show that the hexacoordinated CH₃–Co(Cbl) formation in the *NHP* protonation state follows the same pattern as the reaction in the *NH* protonation state and similar stationary points have been found (Supporting Information for geometries and Table 1 for properties). The barrier for the rate-limiting methyl cation transfer is calculated to be ~16 and ~20 kcal/mol with and without dispersion included, respectively (Table 1, entry 13), which are slightly higher than the corresponding values in the *NH* protonation state (13 and 18 kcal/mol, entry 2 in Table 1). These results show that the deprotonation at the His759–Asp757–Ser810 triad certainly facilitates the CH₃–Co(Cbl) formation, but this effect is not very large.

We further tested the possibility of the deprotonation of the His759–Asp757–Ser810 triad in the *NH* protonation state, that is the deprotonation of the neutral His759. Because the X-ray structure shows a local hydrogen-bonding net in the His759–Asp757–Ser810 triad,⁵ a hydrogen bond is conserved between the His759 and the Asp757. Therefore, if the His759 deprotonation happens, it is the Asp757 that takes the proton from the His759. We thereby tried to optimize the complex with His759 imidazole anion and Asp757 acid in the triad, but it was found that the proton always went back from the Asp757 to the His759 during optimizations. This indicates that the deprotonation of the neutral His759 is impossible. Another deprotonation possibility is the proton release from a protonated His759 cation.

Methyl Radical Transfer Mechanism. As introduced above, a methyl radical transfer mechanism (mechanism ii) has been proposed for the CH₃–Co(Cbl) formation in MetH. This mechanism involves a one electron transition from the Co(I) atom to the CH₃–THF substrate, which leads to a complex of [•]Co(II)Cbl with a CH₃–THF[•] radical. However, there is no direct evidence for this electron transfer yet. In the present work, we also failed in optimizing the singlet-state complex of [•]Co(II)Cbl and CH₃–THF[•] radical in either the *NH* or *N* protonation states, although many attempts were made. In addition, a number of investigations on the methyl transfer in another methyltransferase, methyltetrahydrofolate corrinoid-iron–sulfur protein (CFeSP) methyltransferase (MeTr), showed the absence of either a Co(II) intermediate or an electron transfer process during the catalysis.^{53,54} With this, the proposed radical transfer mechanism including an electron transfer from Co(I) to CH₃–THF seems to be unfavorable for the first half reaction in MetH.

In the calculations, we obtained a triplet-state enzyme–substrate complex in the *NH* protonation state (**React**_{NH}(T), Figure 9), which lies 8.4 kcal/mol (8.6 kcal/mol with dispersion included, entry 17 in Table 1) higher than the singlet closed-shell **React**_{NH} of Figure 4. It turns out that the **React**_{NH}(T) derives from the **React**_{NH} through a single electron transition from Co(I) to the π* orbital of the Cbl corrin. To inspect the possibility of the CH₃–Co(Cbl) formation from a triplet [•]Co(II)Cbl[•] state, we took the **React**_{NH}(T) as the starting point and optimized the stationary points on the triplet-state pathway. The geometries and properties for the stationary points obtained for the triplet state are given in Figure 9 and Table 1, respectively. It can be noticed that the reaction in the triplet state also follows a stepwise pathway, that is a methyl transfer followed by His759

binding. The nature of the first step has been confirmed to be methyl radical transfer with a spin population of ~0.52 at the transferred methyl carbon in the transition state (**TS1**_{NH}(T)). Thus, the resulting penta- (**Int1**_{NH}(T)) and hexacoordinated (**Int2**_{NH}(T)) CH₃–Co(Cbl) intermediates are the species of CH₃–Co(III)(Cbl[•]) in complex with a H–THF[•] radical. However, the rate-limiting methyl radical transfer is calculated to be significantly endothermic by ~15 kcal/mol (~15 kcal/mol with dispersion included, entry 19 in Table 1), with a very large barrier of ~31 kcal/mol (~28 kcal/mol with dispersion included, entry 18 in Table 1). It is thus clear that the methyl radical transfer in the triplet state can also be ruled out as a possibility for the CH₃–Co(Cbl) formation in MetH.

CONCLUSIONS

In this article, we have reported a theoretical investigation of the mechanism of the first half reaction in cobalamin-dependent methionine synthase (MetH), where a CH₃–Co(III)Cbl species is formed. The investigation was performed with a chemical model built on the basis of two X-ray crystal structures (PDB Code: 1BMT⁵ and 1Q8J⁷). Transition states and intermediates along various reaction pathways were optimized and characterized.

The calculations show that the CH₃–Co(III)Cbl formation proceeds via a stepwise pathway, that is a methyl cation transfer from the protonated CH₃–THF substrate to the Co(I)cobalamin, followed by His759 binding to the Co. The former methyl transfer step is found to be rate-limiting with a barrier of 18 kcal/mol. With dispersion included, the reaction barrier is reduced to ~13 kcal/mol (Table 1, entry 2). The protonation at the methyl-bound nitrogen (N_m) of the substrate results in a tetrahedral configuration of N_m and weakens the bond between the N_m and the methyl carbon (C_m), thus facilitating the cleavage of the N_m–C_m bond. Without this protonation, the methyl transfer is shown to be inaccessible (the barrier is ~38 kcal/mol with dispersion included, entry 7 in Table 1), indicating that the indispensable proton uptake must occur before or simultaneously with the methyl transfer. In addition, it has been demonstrated that the deprotonation of the α-face His759–Asp757–Ser810 triad slightly facilitates the CH₃–Co(III)Cbl formation.

The alternative mechanism of methyl radical transfer in the first half reaction of MetH has also been examined in the present article. However, our calculations did not give any support for this mechanism. We further considered the possibility of methyl radical transfer in the triplet state, but it could be ruled out since this kind of reaction is predicted to be endothermic by ~24 kcal/mol (with dispersion included), with a very high barrier of ~37 kcal/mol (Table 1, entries 19 and 18, respectively).

Although a charge separation takes place along the reaction pathway, the solvation effects for most of stationary points are small (Table S1 in Supporting Information). In particular, the energy difference for the **TS1**_{NH} (the transition state for methyl cation transfer) with and without the solvation effect is only 1.1 kcal/mol. This indicates that the present model which includes all key charged groups, to a high degree, captures the chemistry that takes place at the enzyme active site.

Calculations of the homolytic Co–C bond dissociation energy (BDE) for the hexacoordinated methyl-Co(III)Cbl species clearly reveal that the lack of dispersion is responsible for most of the discrepancy of 10–20 kcal/mol between theory and

experiment in previous hybrid DFT computations^{37–40} and the rest of the error originates from an exaggeration of exact exchange in B3LYP. It is shown that the use of the B3LYP* functional coupled with empirical dispersion corrections is a better choice than the nonhybrid BP86 functional for theoretical investigations of Cbl-dependent enzyme reactions. This and other results lead to the conclusion that dispersion (vdW effects) may make non-negligible contributions to the energetics of enzyme reactions, especially for the ones involving at least one large reacting fragment approaching or departing, like in the present case of MetH.

■ ASSOCIATED CONTENT

Supporting Information. B3LYP Co–C bond dissociation energy for CH₃–Co(Cbl); schematic potential energy profile for scanning the N–Co distance of the enzyme–substrate complex (**React_{NH}**) in the NH protonation state; complete ref 25; Solvation effects for stationary points in the CH₃–Co(Cbl) formation; Cartesian coordinates and absolute energies of all optimized structures. This material is available free of charge via the Internet at <http://pubs.acs.org>.

■ AUTHOR INFORMATION

Corresponding Author

*E-mail: shlchen@physto.se (S.-L.C.); Tel.: +46-8-161263, Fax: +46-8-153679, E-mail: ps@physto.se

■ ACKNOWLEDGMENT

This work is supported by the Carl Trygger Foundation.

■ REFERENCES

- Brown, K. L. *Chem. Rev.* **2005**, *105*, 2075–2149.
- Banerjee, R.; Ragsdale, S. W. *Annu. Rev. Biochem.* **2003**, *72*, 209–247.
- Banerjee, R. V.; Matthews, R. G. *FASEB J.* **1990**, *4*, 1450–1459.
- Matthews, R. G. *Acc. Chem. Res.* **2001**, *34*, 681–689.
- Drennan, C. L.; Huang, S.; Drummond, J. T.; Matthews, R. G.; Ludwig, M. L. *Science* **1994**, *266*, 1669–1674.
- Koutmos, M.; Pejchal, R.; Bomer, T. M.; Matthews, R. G.; Smith, J. L.; Ludwig, M. L. *Proc. Natl. Acad. Sci. U.S.A.* **2008**, *105*, 3286–3291.
- Evans, J. C.; Huddler, D. P.; Hilgers, M. T.; Romanchuk, G.; Matthews, R. G.; Ludwig, M. L. *Proc. Natl. Acad. Sci. U.S.A.* **2004**, *101*, 3729–3736.
- Doukov, T.; Hemmi, H.; Drennan, C. L.; Ragsdale, S. W. *J. Biol. Chem.* **2007**, *282*, 6609–6618.
- Liptak, M. D.; Brunold, T. C. *J. Am. Chem. Soc.* **2006**, *128*, 9144–9156.
- Wirt, M. D.; Sagi, I.; Chance, M. R. *Biophys. J.* **1992**, *63*, 412–417.
- Giorgetti, M.; Ascone, I.; Berrettoni, M.; Conti, P.; Zamponi, S.; Marassi, R. *J. Biol. Inorg. Chem.* **2000**, *5*, 156–166.
- Datta, S.; Koutmos, M.; Patridge, K. A.; Ludwig, M. L.; Matthews, R. G. *Proc. Natl. Acad. Sci. U.S.A.* **2008**, *105*, 4115–4120.
- Bandarian, V.; Patridge, K. A.; Lennon, B. W.; Huddler, D. P.; Matthews, R. G.; Ludwig, M. L. *Nat. Struct. Biol.* **2002**, *9*, 53–56.
- Dorweiler, J. S.; Finke, R. G.; Matthews, R. G. *Biochemistry* **2003**, *42*, 14653–14662.
- Liptak, M. D.; Fleischhacker, A. S.; Matthews, R. G.; Brunold, T. C. *Biochemistry* **2007**, *46*, 8024–8035.
- Smith, A. E.; Matthews, R. G. *Biochemistry* **2000**, *39*, 13880–13890.
- Jarrett, J. T.; Choi, C. Y.; Matthews, R. G. *Biochemistry* **1997**, *36*, 15739–15748.
- Becke, A. D. *J. Chem. Phys.* **1993**, *98*, 1372–1377.
- Becke, A. D. *J. Chem. Phys.* **1993**, *98*, 5648–5652.
- Lee, C.; Yang, W.; Parr, R. G. *Phys. Rev. B* **1988**, *37*, 785–789.
- Jaguar, version 7.0, Schrodinger, LLC: New York, NY, 2007.
- Hehre, W. J.; Ditchfield, R.; Pople, J. A. *J. Chem. Phys.* **1972**, *56*, 2257–2261.
- Franci, M. M.; Pietro, W. J.; Hehre, W. J.; Binkley, J. S.; Gordon, M. S.; DeFrees, D. J.; Pople, J. A. *J. Chem. Phys.* **1982**, *77*, 3654–3665.
- Hay, P. J.; Wadt, W. R. *J. Chem. Phys.* **1985**, *82*, 299–310.
- Frisch, M. J. et al. *Gaussian 03*, Rev. D.01; Gaussian, Inc.: Wallingford CT, 2004.
- Tannor, D. J.; Marten, B.; Murphy, R.; Friesner, R. A.; Sitkoff, D.; Nicholls, A.; Ringnalda, M.; Goddard, W. A., III; Honig, B. *J. Am. Chem. Soc.* **1994**, *116*, 11875–11882.
- Marten, B.; Kim, K.; Cortis, C.; Friesner, R. A.; Murphy, R. B.; Ringnalda, M. N.; Sitkoff, D.; Honig, B. *J. Phys. Chem.* **1996**, *100*, 11775–11788.
- Himo, F.; Siegbahn, P. E. M. *Chem. Rev.* **2003**, *103*, 2421–2456.
- Siegbahn, P. E. M. *Q. Rev. Biophys.* **2003**, *36*, 91–145.
- Siegbahn, P. E. M.; Borowski, T. *Acc. Chem. Res.* **2006**, *39*, 729–738.
- Himo, F. *Theor. Chem. Acc.* **2006**, *116*, 232–240.
- Reiher, M.; Salomon, O.; Hess, B. A. *Theor. Chem. Acc.* **2001**, *107*, 48–55.
- Salomon, O.; Reiher, M.; Hess, B. A. *J. Chem. Phys.* **2002**, *117*, 4729–4737.
- Grimme, S. *J. Comput. Chem.* **2004**, *25*, 1463–1473.
- Grimme, S. *J. Comput. Chem.* **2006**, *27*, 1787–1799.
- ORCA, An ab initio, DFT, and semiempirical electronic structure package developed by Frank Neese, Version 2.6, Revision 71, Lehrstuhl fuer Theoretische Chemie, Institut fuer Physikalische und Theoretische Chemie, Universitaet Bonn, Germany.
- Andruniow, T.; Zgierski, M. Z.; Kozlowski, P. M. *J. Am. Chem. Soc.* **2001**, *123*, 2679–2680.
- Kozlowski, P. M.; Zgierski, M. Z. *J. Phys. Chem. B* **2004**, *108*, 14163–14170.
- Kuta, J.; Patchkovskii, S.; Zgierski, M. Z.; Kozlowski, P. M. *J. Comput. Chem.* **2006**, *27*, 1429–1437.
- Jensen, K. P.; Ryde, U. *J. Phys. Chem. A* **2003**, *107*, 7539–7545.
- Siegbahn, P. E. M.; Blomberg, M. R. A.; Chen, S. –L. *J. Chem. Theory Comput.* **2010**, *6*, 2040–2044.
- Dölker, N.; Morreale, A.; Maseras, F. *J. Biol. Inorg. Chem.* **2005**, *10*, 509–517.
- Dölker, N.; Maseras, F.; Lledós, A. *J. Phys. Chem. B* **2003**, *107*, 306–315.
- Jensen, K. P. *Inorg. Chem.* **2008**, *47*, 10357–10365.
- Martin, B. D.; Finke, R. G. *J. Am. Chem. Soc.* **1990**, *112*, 2419–2420.
- Martin, B. D.; Finke, R. G. *J. Am. Chem. Soc.* **1992**, *114*, 585–592.
- Jensen, K. P.; Ryde, U. *ChemBioChem* **2003**, *4*, 413–424.
- Bandarian, V.; Matthews, R. G. *Biochemistry* **2001**, *40*, 5056–5064.
- Randaccio, L.; Furlan, M.; Geremia, S.; Šlouf, M.; Srnova, I.; Toffoli, D. *Inorg. Chem.* **2000**, *39*, 3403–3413.
- Rovira, C.; Biarnés, X. *Inorg. Chem.* **2004**, *43*, 6628–6632.
- Andruniow, T.; Jaworska, M.; Lodowski, P.; Zgierski, M. Z.; Dreos, R.; Randaccio, L.; Kozlowski, P. M. *J. Chem. Phys.* **2008**, *129*, 085101–14.
- Kozlowski, P. M.; Kuta, J.; Galezowski, W. *J. Phys. Chem. B* **2007**, *111*, 7638–7645.
- Zhao, S.; Roberts, D. L.; Ragsdale, S. W. *Biochemistry* **1995**, *34*, 15075–15083.
- Menon, S.; Ragsdale, S. W. *J. Biol. Chem.* **1999**, *274*, 11513–11518.